APOE Isoforms Control Pathogenic Subretinal Inflammation in Age-Related Macular Degeneration

Olivier Levy, Sophie Lavalette, Shulong Hu, Michael Housset, William Raoul, Chiara Eandi, José-Alain Sahel, Patrick Sullivan, Xavier Guillonneau, Florian Sennlaub

The Journal of Neuroscience

http://jneurosci.msubmit.net

JN-RM-2468-15R1

APOE-isoforms control pathogenic subretinal inflammation in age related macular degeneration.

Florian Sennlaub, Institut de la vision
Olivier Levy, Institut de la Vision
Sophie Lavalette, Institut de la vision
Shulong J HU, Instiut de la vision
Chiara Eandi, 5Department of Surgical Sciences, Eye Clinic, University of Torino
Michael Housset, Institut de la Vision
William Raoul, Institut de la Vision
José-Alain Sahel, Institut de la Vision, INSERM UMR_S968, CNRS UMR_7210, Université Pierre et Marie Curie Paris 06
Patrick Sullivan, Duke University Medical Center
Xavier Guillonneau, Institut de la vision

Commercial Interest:

APOE-isoforms control pathogenic subretinal inflammation in age related macular degeneration.

Olivier Levy[1,2,3], Sophie Lavalette[1,2,3], Shulong J. Hu[1,2,3], Michael Housset[1,2,3], William Raoul[1,2,3], Chiara Eandi[5], José-Alain Sahel[1,2,3,4], Patrick M. Sullivan[6], Xavier Guillonneau[1,2,3] and Florian Sennlaub[1,2,3]

[1]Inserm, U 968, Paris, F-75012, France

[2]Sorbonne Universités, UPMC Univ Paris 06, UMR_S 968, Institut de la Vision, Paris, F-75012, France

[3]CNRS, UMR_7210, Paris, F-75012, France

[4] Centre Hospitalier National d'Ophtalmologie des Quinze-Vingts, INSERM-DHOS CIC 503, Paris, F-75012, France

[5]Department of Surgical Sciences, Eye Clinic, University of Torino, Torino, Italy.

[6]Department of Medicine, Centers for Aging and Geriatric Research Education and Clinical Center, Durham Veteran Affairs Medical Center, Duke University, Durham, North Carolina 27710.

†Correspondence should be addressed to Dr Florian Sennlaub, Inserm, UMR_S 968, Institut de la Vision, Paris, F-75012, France. Tel: (33) 1 53 46 26 93,

Email: florian.sennlaub@inserm.fr.

Number of pages: 33

Number of figures: 5

Number of words:

Abstract: 185

Introduction: 604

Discussion: 1357

Conflict of interest: The authors declare no competing financial interests

Acknowledgments:

This work was supported by grants from INSERM, ANR Maladies Neurologiques et Psychiatriques (ANR- 08-MNPS -003), ANR Geno 2009 (R09099DS), Labex Lifesenses, Carnot, and ERC starting Grant (ERC-2007 St.G. 210345) and by Association de Prévoyance Santé de ALLIANZ.

Abstract :

Contrary to Alzheimers disease (AD), the *APOE2*-allele increases and the *APOE4*-allele reduces the risk to develop age related macular degeneration (AMD) compared to the most common *APOE3*-allele. The underlying mechanism for this association with AMD and the reason for the puzzling difference with AD are unknown. We previously demonstrated that pathogenic subretinal mononuclear phagocytes (MP) accumulate in *Cx3cr1*-deficient mice due to the overexpression of APOE, IL-6 and CCL2. We here show using targeted replacement mice expressing the human APOE isoforms (TRE2, TRE3, and TRE4) that MPs of *TRE2*-mice express increased levels of APOE, IL-6, and CCL2 and develop subretinal MP accumulation, photoreceptor degeneration and exaggerated choroidal neovascularization similar to AMD. Pharmacological inhibition of the cytokine induction inhibited the pathogenic subretinal inflammation. In the context of APOE-dependent subretinal inflammation in $Cx3cr1^{GFP/GFP}$-mice, the *APOE4*-allele led to diminished APOE and CCL2 levels and protected $Cx3cr1^{GFP/GFP}$-mice against harmful subretinal MP accumulation observed in $Cx3cr1^{GFP/GFP}TRE3$ mice. Our study shows that pathogenic subretinal inflammation is APOE isoform-dependent and provides rationale for the previously unexplained implication of the APOE2-isoform as a risk factor and the APOE4-isoform as a protective factor in AMD pathogenesis.

Significance statement:

The understanding of how genetic predisposing factors, that play a major role in AMD, participate in its pathogenesis is an important clue to decipher the patho-mechanism and develop efficient therapies. In this study, we used transgenic, targeted replacement mice that carry the three human APOE-isoform-defining sequences at the mouse APOE chromosomal location and express the human APOE-isoforms. Our study is the first to show how *APOE2* provokes and *APOE4* inhibits the cardinal AMD features, inflammation, degeneration and exaggerated neovascularization. Our findings reflect the clinical association of the genetic predisposition that was recently confirmed in a major pooled analysis. They emphasize the role of APOE in inflammation and inflammation in AMD.

Introduction:

In humans, the *APOE* gene has three common genetic variants (*APOE2, APOE3,* and *APOE4)*, due to two polymorphisms rs7412 and rs429358 that are imbedded in a well-defined CpG island, and lead to two cysteine-arginine interchanges at residues 112 and 158 (Yu et al., 2013). The *APOE2*-allele is associated with higher APOE concentrations in plasma, cerebrospinal fluid and the brain tissue (Riddell et al., 2008; Bales et al., 2009) due to impaired clearance caused by APOE2's decreased affinity for the LDL receptor (Mahley and Rall, 2000). Its transcription can also be increased in certain cell types (astrocytes, neurons) due to the loss of CpG sites associated with *APOE3* and *APOE4*-alleles (Yu et al., 2013). Compared to the *APOE3*-allele, the *APOE4*-allele is transcribed similarly in neurons and astrocytes (Yu et al., 2013), but its protein concentration in plasma, the CSF and in brain parenchyma are decreased (Riddell et al., 2008; Bales et al., 2009; Sullivan et al., 2011). The structural changes in the APOE4 protein also lead to diminished association with HDL (Dong and Weisgraber, 1996) and impaired reverse cholesterol transport (Heeren et al., 2004; Mahley et al., 2009).

APOE2-allele carriers are at increased risk for developing late age-related macular degeneration (AMD, odds ratio (OR) = 1.83 for homozygote *APOE2*-allele carriers) and are protected against Alzheimer's disease (AD), while the *APOE4*-allele protects against AMD (OR = 0.72 per haplotype) and is a risk factor for AD compared to the most common *APOE3*-allele (Mahley and Rall, 2000; McKay et al., 2011). This association was recently confirmed in a pooled study of over 20 000 subjects (McKay et al., 2011). It is found for both clinical forms of late AMD: wet AMD, which is defined by choroidal neovascularization (CNV) and geographic atrophy (GA), which is characterized by an extending lesion of both the retinal

pigment epithelium (RPE) and photoreceptors. In AD, the *APOE4*-allele is associated with greater β-amyloid burden, possibly due to reduced efficacy in clearance of β-amyloid clearance via multiple pathways (Bales et al., 2009; Mahley et al., 2009). The mechanism underlying the associations of the APOE-isoforms with AMD remain unexplained.

APOE is the main lipoprotein of the brain and the retina (Mahley and Rall, 2000; Anderson et al., 2001). It is strongly expressed in mononuclear phagocytes (MPs), such as macrophages and microglial cells (Peri and Nusslein-Volhard, 2008; Levy et al., 2015) and plays a major role in macrophage lipid efflux and reverse cholesterol transport in conjunction with APOA-I (Mahley and Rall, 2000; Mahley et al., 2009). APOE and APOA-I can also induce IL-6 and CCL2 in MPs the absence of pathogen-derived ligands (Smoak et al., 2010; Levy et al., 2015).

We recently showed that subretinal MPs that accumulate in AMD, strongly express APOE (Levy et al., 2015). The subretinal MPs of *Cx3cr1*$^{GFP/GFP}$-mice that develop subretinal inflammation and cardinal features of AMD (Combadiere et al., 2007), express similar high levels of APOE (Levy et al., 2015), but also IL-6 (Levy et al., 2015) and CCL2 (Sennlaub et al., 2013). We showed that APOE-induced IL-6 release from MPs represses RPE immune-suppression, prolongs subretinal MP survival, and promotes subretinal inflammation (Levy et al., 2015). Furthermore, we demonstrated that increased levels of CCL2 in *Cx3cr1*$^{GFP/GFP}$-mice recruit pathogenic inflammatory CCR2^{+} monocytes to the subretinal space (Sennlaub et al., 2013). In consequence, subretinal pathogenic MPs accumulate in *Cx3cr1*$^{GFP/GFP}$-mice due to increased MP recruitment and decreased MP elimination. *ApoE* deletion in *Cx3cr1*$^{GFP/GFP}$-mice prevented age- and stress-induced subretinal MP accumulation, and reduced associated CNV (Levy et al., 2015).

111 We here investigated the influence of the APOE alleles and isoforms on subretinal
112 inflammation and associated photoreceptor degeneration and choroidal neovascularization,
113 major hallmarks of AMD.
114

Materials and Methods:

Animals

Targeted replacement mice that express human APOE isoforms (TRE2,3, and 4) were engineered as previously described (Sullivan et al., 1997) and provided as a generous gift by Dr. Patrick Sullivan, backcrossed with C57BL/6 mice to eliminate the Crb1^{rd8} contamination in the three strains and crossed to Cx3cr1$^{GFP/GFP}$mice (Charles River). Mice were housed in the animal facility under specific pathogen-free condition, in a 12/12h light/dark (100-500 lux) cycle with water and normal diet food available ad libitum. All experimental protocols and procedures were approved by the local animal care ethics committee "Comité d'éthique en expérimentation animale Charles Darwin" (Ce5/2010/013; Ce5/2011/033; Ce5/2010/044). We used male mice for choroidal neovascularization experiments, whereas experiments on aged and light-challenged mice were performed on mice of either sex, as we did not observe differences between the sexes in these conditions.

Light-challenge and laser-injury model

Two- month-old mice of either sex were adapted to darkness for 6 hours, pupils dilated and exposed to constant green LED light (starting at 2AM, 4500 Lux, JP Vezon equipements) for 4 days as previously described (Sennlaub et al., 2013). Laser-coagulations were performed on male mice with a 532nm ophthalmological laser mounted on an operating microscope (Vitra Laser, 532 nm, 450 mW, 50 ms and 250 µm) as previously described (Levy et al., 2015). Intravitreal injections of 2µl of PBS, isotype control rat IgG1, and rat anti-mouse CD14 (BD Biosciences) were performed using glass capillaries (Eppendorf) and a microinjector. The 2µl solution of the antibodies were injected at 50µg/ml, corresponding to an intraocular concentration of 5µg/ml assuming their dilution by approximately 1/10th in the intra-ocular volume.

Immunohistochemistry, CNV and MPs quantification and histology

RPE and retinal flatmounts were stained and quantified as previously described (Sennlaub et al., 2013) using polyclonal rabbit anti- IBA-1 (Wako) and rat anti-mouse CD102 (clone 3C4, BD Biosciences) appropriate secondary antibodies and counterstained with Hoechst if indicated. Preparations were observed with fluorescence microscope (DM5500, Leica). Histology of mice eyes and photoreceptor quantification were performed as previously described (Sennlaub et al., 2013).

Cell preparations and cell culture

In accordance with the Declaration of Helsinki, volunteers provided written and informed consent for the human monocyte expression studies, which were approved by the Centre national d'ophthalmologie des Quinze-Vingt hospital (Paris, France) ethics committees (no. 913572). PBMCs were isolated from heparinized venous blood from healthy volunteer individuals by 1-step centrifugation on a Ficoll Paque layer (GE Healthcare) and sorted with EasySep Human Monocyte Enrichment Cocktail without CD16 Depletion Kit (StemCells Technology). Mouse peritoneal macrophages, bone marrow-derived monocytes and photoreceptor outer segment (POS) isolation (all in serum-free X-Vivo 15 medium) were performed as previously described (Sennlaub et al., 2013). In specific experiments, cells were stimulated with the different recombinant human APOE isoforms (5µg/ml, Leinco Technologies), recombinant human APOE3 90 minutes heat-denatured (5µg/ml, Leinco Technologies), APOE3 (5µg/ml) with LPS inhibitor Polymyxin B (25µg/ml, Calbiochem), rat anti-IgG isotype control (25µg/ml, R&D), rat anti-mouse CD14 (25µg/ml, R&D), mouse anti-IgG isotype control (25µg/ml), mouse anti-human TLR2 (25µg/ml, Invivogen), human IgA2 isotype control (25µg/ml, Invivogen), human anti-human TLR4 (25µg/ml, Invivogen) and POS prepared as previously described (Sennlaub et al., 2013).

Reverse transcription and real-time polymerase chain reaction and ELISA

IL-6, CCL2, and IL-1β RT-PCRs using Sybr Green (Life Technologies) and ELISAs using mouse or human IL-6 DuoSet (R&D Systems), mouse or human CCL2 Duoset (R&D) and human APOE Pro kit (Mabtech) were performed as previously described (Sennlaub et al., 2013; Levy et al., 2015; Hu et al., 2015).

Statistical analysis

Graph Pad Prism 5 (GraphPad Software) was used for data analysis and graphic representation. All values are reported as mean ± SEM. Statistical analysis was performed by one-way or two-way Anova analysis of variance followed by Dunnetts post-test or Mann–Whitney test for comparison among means depending on the experimental design. The *p*-values are indicated in the figure legends.

Results:

The APOE2 allele leads to age- and stress-related subretinal MP accumulation, retinal degeneration, and exacerbated choroidal neovascularization

The subretinal space, located between the retinal pigment epithelium (RPE) and the photoreceptor outer segments (POS), does not contain significant numbers of mononuclear phagocytes (MPs) under normal conditions (Penfold et al., 2001 ; Gupta et al., 2003 ; Combadiere et al., 2007; Levy et al., 2015). This is likely the result of physiologically low levels of chemoattractants along with strong immunosuppressive RPE signals that quickly eliminate infiltrating MPs (Sennlaub et al., 2013 ; Levy et al., 2015). We have previously shown that the lack of the tonic inhibitory CX3CL1/CX3CR1 signal, observed in *Cx3cr1*-deficient mice, is sufficient to induce pathogenic chronic subretinal MP accumulation as a consequence of increased recruitment and decreased elimination (Combadiere et al., 2007; Sennlaub et al., 2013; Levy et al., 2015). We showed that this accumulation is dependent on the over-expression of APOE in *Cx3cr1*-deficient MPs (Levy et al., 2015). To evaluate a potential role of the human APOE isoforms in subretinal inflammation we used targeted replacement mice expressing human isoforms (TRE2, TRE3, and TRE4) (Sullivan et al., 1997). We first backcrossed the strains with C57BL/6J mice to eliminate the *Crb1*^{rd8} contamination in the three strains, that can lead to AMD like features (Mattapallil et al., 2012). The mice were raised under 12-h light/12-h dark cycles at 100-500 lux at the cage level, with no additional cover in the cage, the conditions that induce MP accumulation in *Cx3cr1*-deficient mice with age (Combadiere et al., 2007). Quantification of subretinal IBA-1^{+}MPs on retinal and RPE/choroidal-flatmounts of 2m- and 12m-old TRE2, 3, and 4 mice revealed that TRE2 mice develop age-dependent subretinal MP accumulation compared to

TRE3 and TRE4 mice (Fig. 1A). Similarly, TRE2-mice accumulated significantly more subretinal MPs after a four-day light-challenge and the MPs continued to accumulate after return for 10 additional days in normal light conditions (Fig. 1B, the intensity of our light-challenge model used herein was calibrated to induce subretinal inflammation in inflammation-prone *Cx3cr1*$^{GFP/GFP}$-mice but not in *WT* mice (Sennlaub et al., 2013)).

We also observed a thinning of the outer nuclear layer (ONL) that contains the photoreceptor nuclei on histological retinal sections from 12m-old *TRE2*-mice compared to *TRE3*-mice (Fig. 1C, micrographs taken at equal distance from the optic nerve). Photoreceptor nuclei row counts (Fig. 1C') and calculation of the area under the curve (Fig. 1C'') revealed that the age-related accumulation of subretinal MPs in *TRE2-mice* is associated with significant photoreceptor cell loss when compared to *TRE3*-, and *TRE4*-mice.

In addition, subretinal IBA-1^{+}MPs (green staining, counted on the RPE at a distance of 0-500µm to CD102^{+}CNVs, red staining) were significantly more numerous in *TRE2* mice seven days after a laser-impact (Fig. 1D), and had developed significantly greater CNV lesions (Fig.1E) compared to the other strains.

Taken together, our data demonstrate that *TRE2*-mice, expressing the *APOE2*-AMD-risk allele, develop age-related subretinal inflammation and photoreceptor degeneration and exaggerated inflammation and CNV after laser-injury similar to late AMD.

The APOE2-allele increases APOE levels in the eye and APOE transcription and IIRC activation in MPs.

We previously showed that the levels of soluble APOE are elevated in adult *TRE2* mouse brains and diminished in *TRE4* brains compared to *TRE3* mice in a model of Alzheimers disease (Bales et al., 2009). Similarly, ELISA analysis of APOE levels of homogenates of PBS-perfused posterior segments (retina and RPE/choroid plexus) of 12-

month-old mice revealed significantly higher levels of APOE in *TRE2*-mice compared to *TRE3*- and *TRE4*-mice (Fig. 2A). Furthermore, immunohistochemical localization of APOE on retinal flatmounts of *TRE2*-mice (Fig 2B, red staining) revealed strong APOE expression in subretinal IBA-1^{+}MPs (Fig. 2B, green staining).

The polymorphism rs7412 that defines the APOE2 isoform also leads to the loss of a CpG site in the *APOE2*-allele that has been shown to moderately, but significantly, increase *APOE* transcription in brain astrocytes, but not in hepatocytes (Yu et al., 2013). Our data confirms that APOE transcription in hepatocytes does not differ between genotypes (Yu et al., 2013) (Fig. 2C, rtPCR;) and that APOE concentrations in the blood were significantly increased in *TRE2*-mice (Fig. 2D, blood plasma ELISA), shown to be due to its decreased clearance rate (Mahley and Rall, 2000). However, bone-marrow derived monocytes (cultured with photoreceptor outer segments for three days to mimic subretinal macrophage differentiation) (Fig. 2E, rtPCR) and peritoneal macrophages (Fig. 2F, rtPCR) from *TRE2*-mice transcribed signifivantly higher levels of *ApoE* mRNA compared to MPs of the other mouse strains. Accordingly, the APOE secretion of *TRE2*-mice macrophages was robustly increased (Fig. 2G, ELISA of supernatant), compared to the other groups.

APOE and APOA-I have been shown to activate the TLR2-TLR4-CD14-dependent innate immunity receptor cluster (IIRC) in mouse peritoneal macrophages in the absence of pathogen-derived ligands and to induce inflammatory cytokines such as IL-6 (Smoak et al., 2010; Levy et al., 2015), but also CCL2 (shown for APOA-I(Smoak et al., 2010)). We here show that human blood derived CD14+monocytes significantly secrete IL6 after 24h of recombinant lipid-free APOE3 stimulation (Fig. 2H) similar to mouse macrophages. 90min heat-denaturation completely abolished the induction, while the LPS inhibitor Polymyxin B did not, confirming that LPS contamination of APOE3 is not accountable for the effect, as shown for APOA-I using multiple approaches (Smoak et al., 2010). This induction was due to

the activation of the CD14/TLR2/TLR4-dependent IIRC, as neutralizing antibodies to CD14, TLR2, and TLR4 inhibited this effect, when compared to control antibodies (Fig. 2H). Accordingly, peritoneal macrophages from *TRE2*-mice that express increased amounts of APOE (Fig. 2C and D), also transcribed significantly more IL-6, CCL2, and IL-1β compared to macrophages of the other isoforms (Fig. 2I).

Taken together, our results show that the *APOE2*-allele increases APOE levels in the tissue and *APOE* expression in MPs. We confirm that APOE activates IIRC and show that the excessive APOE expression in macrophages from TRE2 mice is associated with increased production of inflammatory cytokines *in vitro*.

Figure 3: IIRC-inhibition reduces subretinal MP accumulation and choroidal neovascularization in TRE2-mice in vivo.

To evaluate if increased IIRC activation is implicated in subretinal MP accumulation observed in TRE2-mice in vivo, we inhibited the IIRC by an intravitreal injection of a CD14-neutralizing antibody in the laser-induced CNV model. The antibody, that blocks APOE-dependent cytokine induction (Levy et al., 2015), inhibited subretinal MP accumulation around the laser injury, quantified on IBA1-stained RPE/choroidal flatmounts (Fig. 3A) and $CD102^{+}$CNV formation (Fig. 3B) at d7 after laser-injury of *TRE2*-mice compared to control IgG.

These results confirm that the CD14-dependent inflammatory cytokine induction participates in subretinal MP accumulation in *TRE2*-mice *in vivo*, similar to *Cx3cr1*$^{GFP/GFP}$mice (Levy et al., 2015).

The APOE4-allele protects APOE-overexpressing Cx3cr1$^{GFP/GFP}$mice from subretinal MP accumulation, retinal degeneration and exacerbated choroidal neovascularization.

Cx3cr1 deficient mice lack the tonic inhibitory signal of neuronal CX3CL1, and develop subretinal MP accumulation and concomitant photoreceptor degeneration with age

when raised in cyclic light at 100-500 lux (Combadiere et al., 2007; Chinnery et al., 2011; Sennlaub et al., 2013; Hu et al., 2015; Levy et al., 2015). The accumulation can be prevented by raising the animals in darkness (Combadiere et al., 2007) or in dim light conditions (Luhmann et al., 2013) and be accelerated by a light-challenge (Sennlaub et al., 2013; Hu et al., 2015; Levy et al., 2015)(for more details see the mini review in the supplementary data of Sennlaub et al. (Sennlaub et al., 2013)). Although these features do not mimic all the aspects of AMD (Drusen formation and RPE atrophy) they do model subretinal inflammation and associated photoreceptor degeneration, two hallmarks of AMD (Gupta et al., 2003). *Cx3cr1* deletion also increases subretinal MP accumulation in diabetes (Kezic et al., 2013), in a paraquat-induced retinopathy model (Chen et al., 2013) and in a retinitis pigmentosa model (Peng et al., 2014). We previously demonstrated that pathogenic MP accumulate in *Cx3cr1*-deficient mice due to the overexpression of APOE, IL-6 and CCL2 (Sennlaub et al., 2013; Levy et al., 2015). To evaluate a possible influence of the APOE4 isoform in a model of pathological subretinal inflammation, we crossed *TRE3*- and *TRE4*-mice to $Cx3cr1^{GFP/GFP}$-mice. (Levy et al., 2015)

Quantification of subretinal IBA-1^{+}MPs on retinal and RPE/choroidal-flatmounts of 2m- and 12m-old $Cx3cr1^{GFP/GFP}TRE3$-mice and $Cx3cr1^{GFP/GFP}TRE4$-mice mice revealed that the age-dependent subretinal MP accumulation observed in $Cx3cr1^{GFP/GFP}TRE3$-mice was prevented in $Cx3cr1^{GFP/GFP}TRE4$-mice (Fig. 4A). A 4-day light-challenge led to similar initial subretinal MP accumulation, but the increase of MPs after return to normal light conditions was significantly blunted in $Cx3cr1^{GFP/GFP}TRE4$-mice compared to $Cx3cr1^{GFP/GFP}TRE3$-mice (Fig. 4B).

Furthermore, micrographs of histological sections of 12m-old mice, revealed a thicker outer nuclear layer (ONL) in $Cx3cr1^{GFP/GFP}TRE4$-mice compared to the thinned $Cx3cr1^{GFP/GFP}TRE3$-mice (Fig. 4C). Photoreceptor nuclei row counts (Fig. 4C') and

298 calculation of the area under the curve (Fig. 4C'') shows that the inhibition of the age-related
299 accumulation of subretinal MPs in *Cx3cr1*$^{GFP/GFP}$*TRE4*-mice compared to
300 *Cx3cr1*$^{GFP/GFP}$*TRE3*-mice significantly inhibited the associated photoreceptor cell loss. Please
301 note that the age-related subretinal MP accumulation and photoreceptor degeneration
302 observed in *Cx3cr1*$^{GFP/GFP}$*TRE3*-mice are significantly increased compared to *TRE3*-mice
303 presented in Fig. 1, similar to *Cx3cr1*$^{GFP/GFP}$-mice expressing mouse APOE (Sennlaub et al.,
304 2013) (MP/mm^2 of 12-months old mice: *TRE3*-mice: 7.315+/-1.72SEM, *Cx3cr1*$^{GFP/GFP}$*TRE3*-
305 mice: 16.6+/-2.22SEM; Area under the curve: *TRE3*-mice: 148.3+/-1.52SEM,
306 *Cx3cr1*$^{GFP/GFP}$*TRE3*-mice: 137.3+/-2.12SEM).

307 Moreover, laser-induced subretinal IBA-1$^+$MPs in 2-months old mice (green staining)
308 adjacent to CD102$^+$CNVs (red staining) was again significantly inhibited in
309 *Cx3cr1*$^{GFP/GFP}$*TRE4*-mice compared to *Cx3cr1*$^{GFP/GFP}$*TRE3*-mice (Fig. 4D) and had developed
310 significantly greater CNV lesions at 14days after laser-injury (Fig. 4E) compared to the other
311 strains.

312 In summary, our data demonstrates that the *APOE4*-allele, which is protective for
313 AMD, inhibits subretinal inflammation and concomitant degeneration and CNV in Cx3cr1-
314 deficiency compared to *APOE3*.

315 ***The APOE4-allele decreases ocular APOE levels in Cx3cr1$^{GFP/GFP}$ mice and activates the IIRC***
316 ***inefficiently.***

317 To investigate if the *APOE3* and *APOE4*-allele influence the APOE level in the eyes of
318 *Cx3cr1*$^{GFP/GFP}$*TRE*-mice we analyzed APOE levels of homogenates of PBS-perfused posterior
319 segments (retina and RPE/choroid plexus) of 12-month-old mice. APOE levels were
320 significantly lower in homogenates of 12-month-old *Cx3cr1*$^{GFP/GFP}$*TRE4*-mice compared to

Cx3cr1$^{GFP/GFP}$*TRE3*-mice (Fig. 5A), similar to APOE levels in the eyes of TRE mice (see above) and brains of PDAPP mice expressing human APOE isoforms (Bales et al., 2009).

APOA-I and APOE likely activate the IIRC by modifying the cholesterol content of the lipid rafts in which they are located (Smoak et al., 2010). As the APOE4 isoform has an impaired capacity to promote cholesterol efflux and transport (Heeren et al., 2004; Mahley et al., 2009), we next tested its ability to activate the IIRC of blood-derived human monocytes in culture. Interestingly, stimulation of monocytes for 24h by recombinant APOE4 induced significantly less IL-6 and CCL2 secretion compared to the induction of the cytokines by equimolar concentrations of APOE3 (Fig. 5B).

APOE transcription (Fig. 5C, rtPCR) and APOE secretion (Fig. 5D, ELISA of supernatant) in peritoneal macrophages from *Cx3cr1*$^{GFP/GFP}$*TRE3*-mice and *Cx3cr1*$^{GFP/GFP}$*TRE4*-mice were comparable, similar to previous reports from astrocytes the *APOE4*-allele did not diminish APOE production (Yu et al., 2013). However, in accordance with a decreased ability to activate the IIRC, peritoneal macrophages from *Cx3cr1*$^{GFP/GFP}$*TRE4*-mice transcribed significantly less *CCL2* compared to macrophages from *Cx3cr1*$^{GFP/GFP}$*TRE3*-mice while the IL-6 transcription was variable, but not significantly different (Fig. 5E).

Taken together, our results show that the *APOE4* allele leads to decreased APOE tissue levels and to a reduced capacity to activate the IIRC and induce CCL2 in MPs.

Discussion:

We have previously shown that the lack of the tonic inhibitory CX3CL1/CX3CR1 signal, observed in Cx3cr1-deficient mice, is sufficient to induce pathogenic chronic subretinal MP accumulation due to increased CCL2-dependent monocyte recruitment and IL-6 dependent decrease of subretinal MP elimination (Combadiere et al., 2007; Sennlaub et al.,

345 2013 ; Hu et al., 2015; Levy et al., 2015). We showed that this accumulation is dependent on
346 the over-expression of APOE in Cx3cr1-deficient MPs (Levy et al., 2015). As the APOE
347 isoforms are associated with significant differences in APOE levels in humans (Mahley and
348 Rall, 2000) and in humanized transgenic mice expressing APOE isoforms (Bales et al., 2009;
349 Yu et al., 2013), we here evaluated the consequences of the three isoforms on chorioretinal
350 homeostasis.

351 Our study shows that *TRE2*-mice, carrying the AMD-risk-allele, develop age-, light-,
352 and laser-induced subretinal mononuclear phagocyte (MP) accumulation associated with
353 photoreceptor degeneration and excessive CNV. *TRE2*-mice displayed increased tissue levels
354 of APOE measured in whole retinal/choroidal protein extracts compared to *TRE3*- and *TRE4*-
355 mice. This increase is likely due to reduced LDLR-dependent APOE2 uptake (Fryer et al.,
356 2005) of APOE that is produced in the RPE, the inner retina and by subretinal MPs (Anderson
357 et al., 2001 ; Levy et al., 2015). Similar to CX3CR1$^{GFP/GFP}$mice and AMD patients (Levy et
358 al., 2015), subretinal MPs in *TRE2*-mice stained strongly positive for APOE. *In vitro*, we
359 show that the *APOE2* allele is associated with increased APOE transcription and secretion in
360 macrophages from *TRE2*-mice, as previously shown for astrocytes (Yu et al., 2013). The
361 APOE-levels in and around subretinal MPs is therefore likely elevated because of increased
362 APOE-transcription and decreased LDLR-dependent clearance in the tissue. It is not yet clear
363 to what extent APOE from non-myeloid cells participate in the subretinal inflammation and
364 whether extracellular or intracellular APOE within the MPs is the determining factor.

365 APOE is capable of activating the CD14/TLR2/TLR4-dependent IIRC and inducing IL-
366 6, as previously shown for mouse macrophages (Smoak et al., 2010; Levy et al., 2015). We
367 here confirm that APOE can induce inflammatory cytokines in a similar manner in human
368 monocytes. Moreover, macrophages from *TRE2*-mice that express significantly higher levels
369 of APOE also transcribed higher levels of inflammatory cytokines, such as IL-6, CCL2, and

370 IL-1β in accordance with an APOE-activation of the IIRC and similar to APOE-
371 overexpressing Cx3cr1-deficient macrophages (Sennlaub et al., 2013; Hu et al., 2015; Levy et
372 al., 2015). We previously showed that CCL2 (Sennlaub et al., 2013) and IL6 (Levy et al.,
373 2015) promote subretinal MP accumulation by increasing monocyte recruitment and
374 decreasing MP clearance respectively. Indeed, inhibition of the IIRC by a CD14-blocking
375 antibody in laser-injured *TRE2*-mice decreased subretinal MP accumulation and
376 neovascularization. These results demonstrate that IIRC activation is significantly involved in
377 the subretinal MP accumulation in *TRE2*-mice *in vivo*. Taken together, *Cx3cr1*$^{GFP/GFP}$-mice
378 and *TRE2*-mice both over-express APOE in mononuclear phagocytes, although for different
379 reasons. In both mouse strains the increased APOE is associated with IIRC activation, CCL2
380 and IL6 induction, and pathogenic subretinal inflammation. Although these features do not
381 mimic all the aspects of AMD (Drusen formation and RPE atrophy) they do model subretinal
382 inflammation and associated photoreceptor degeneration, two hallmarks of AMD (Gupta et
383 al., 2003). We previously demonstrated the importance of APOE in this process, as *APOE*-
384 deletion protected *Cx3cr1*$^{GFP/GFP}$-mice against the inflammation (Levy et al., 2015).
385 Interestingly, increased levels of CCL2 and IL6 are also observed in late AMD (Seddon et al.,
386 2005; Jonas et al., 2010; Sennlaub et al., 2013; Chalam et al., 2014), where chronic MP
387 accumulation is observed (Penfold et al., 2001; Gupta et al., 2003 ; Combadiere et al., 2007;
388 Sennlaub et al., 2013; Levy et al., 2015). The observation that inhibition of subretinal MP
389 accumulation in a variety of animal models represses CNV (Sakurai et al., 2003; Tsutsumi et
390 al., 2003; Liu et al., 2013) and degeneration (Guo et al., 2012; Rutar et al., 2012; Suzuki et al.,
391 2012; Kohno et al., 2013) strongly suggests that chronic subretinal inflammation partakes in
392 AMD pathogenesis.

The chronic non-resolving inflammation in AMD is associated with an increase in APOE (Klaver et al., 1998; Anderson et al., 2001 ; Levy et al., 2015) similar to other inflammatory conditions (Rosenfeld et al., 1993). To evaluate if a potential influence of the protective *APOE4*-allele would become apparent in a situation of increased inflammation and APOE abundance, we crossed *TRE3* and *TRE4*-mice to the APOE-overexpressing *Cx3cr1*$^{GFP/GFP}$-mice. In the inflammatory context of *Cx3cr1*$^{GFP/GFP}$-mice, the *APOE4*-allele led to diminished APOE levels and the *APOE4*-allele protected *Cx3cr1*$^{GFP/GFP}$-mice against harmful subretinal MP accumulation observed in *APOE3* carrying *Cx3cr1*$^{GFP/GFP}$mice. APOE4 is characterized, among others, by its decreased capacity to transport cholesterol compared to APOE3 (Heeren et al., 2004) and might thereby be less capable of modifing the cholesterol content of the lipid rafts and activating IIRC (Smoak et al., 2010). Indeed, our results show that recombinant APOE4 induced less IL-6 and CCL2 compared to equimolar APOE3 concentrations in human monocytes *in vitro*. Similarly, macrophages from *Cx3cr1*$^{GFP/GFP}$*TRE4*-mice transcribed less *CCL2* compared to macrophages from *Cx3cr1*$^{GFP/GFP}$*TRE3*-mice, although their APOE expression was comparable. It is not clear why *Cx3cr1*$^{GFP/GFP}$*TRE4*-macrophages did not differ from *Cx3cr1*$^{GFP/GFP}$*TRE3*-macrophages in terms of *IL-6* transcription levels. Other unknown regulatory elements likely influence the transcription of the individual cytokines in macrophages and the interplay of Cx3cr1-deficiency and the human APOE3 and APOE4 isoform in the mouse macrophages might affect these pathways. We previously showed that CCL2 inhibition in *Cx3cr1*$^{GFP/GFP}$mice significantly inhibited age-, laser- and light-induced subretinal MP accumulation (Sennlaub et al., 2013) and diminished production of CCL2, as a result of reduced APOE concentrations and APOE4s impaired capacity to induce cytokines might explain the reduced inflammation and inhibition of degeneration and CNV observed in *Cx3cr1*$^{GFP/GFP}$TRE4 mice.

417 To our knowledge, this is the first study to describe a comprehensive pathomechanism
418 of the involvement of APOE isoforms in AMD that is in accordance with the clinical
419 observation of the *APOE2*-allele being an AMD-risk factor and the *APOE4*-allele an AMD-
420 protective genetic factor. One previous study demonstrated that *TRE4*-mice on high fat diet
421 develop lipid accumulations in the Bruch's membrane, proposed as similar to early AMD
422 (Malek et al., 2005) and that are also observed in *ApoE*$^{-/-}$-mice (Ong et al., 2001). While these
423 observations might apply to early AMD, they are unlikely to play a role in late AMD in which
424 increased APOE immunoreactivity is observed (Klaver et al., 1998; Anderson et al., 2001;
425 Levy et al., 2015) and in which the *APOE4*-allele plays a protective role (McKay et al., 2011).
426 The involvement of increased reverse cholesterol transport (RCT) in AMD might also be
427 supported by the observation that APOA-I levels are elevated in the vitreous of AMD patients
428 (Koss et al., 2014). Furthermore, a polymorphism of the ATP binding cassette transporter 1
429 (ABCA1, associated with low HDL and therefore possibly impaired RCT) has recently been
430 shown to be protective against advanced AMD (Chen et al., 2010).

431 Our study also sheds an interesting light on the puzzling differences of the APOE-
432 isoform association with AMD (McKay et al., 2011) and AD (Mahley and Rall, 2000), two
433 major age-related neurodegenerative diseases: In AD, the *APOE4*-allele is associated with
434 greater β-amyloid burden, possibly due to decreased APOE tissue concentrations and reduced
435 efficacy in clearance of β-amyloid clearance via multiple pathways (Bales et al., 2009;
436 Mahley et al., 2009). Cx3cr1$^{-/-}$mice that express increased amounts of APOE in all MPs,
437 including MCs (Levy et al., 2015), are protected against beta-amyloid deposition in
438 Alzheimer disease mouse models (Lee et al., 2010). In AMD, we show that excessive APOE
439 expression associated with the AMD-risk *APOE2*-allele leads to the induction of
440 inflammatory cytokines that promote pathogenic subretinal inflammation (Fig1-3 and (Levy

441 et al., 2015)), similar to Cx3cr1$^{-/-}$mice (Combadiere et al., 2007; Sennlaub et al., 2013 ; Peng
442 et al., 2014; Levy et al., 2015). On the other hand we show that the *APOE4*-allele is protective
443 in the context of APOE-overexpression Cx3cr1$^{-/-}$mice (Levy et al., 2015)), due to decreased
444 APOE tissue concentrations (Riddell et al., 2008; Bales et al., 2009; Sullivan et al., 2011) and
445 its reduced capacity to induce inflammatory cytokines (Fig. 4 and 5).

446 Taken together, our study shows that the *APOE2*-allele leads to increased APOE
447 expression, IIRC activation and subretinal inflammation, while the APOE4-allele diminishes
448 IIRC activation and inflammation. Our study provides rationale for the previously
449 unexplained implication of the APOE genotype in AMD, and opens avenues toward therapies
450 inhibiting pathogenic chronic inflammation in late AMD.
451

References:

Anderson DH, Ozaki S, Nealon M, Neitz J, Mullins RF, Hageman GS, Johnson LV (2001) Local cellular sources of apolipoprotein E in the human retina and retinal pigmented epithelium: implications for the process of drusen formation. Am J Ophthalmol 131:767-781.

Bales KR, Liu F, Wu S, Lin S, Koger D, DeLong C, Hansen JC, Sullivan PM, Paul SM (2009) Human APOE isoform-dependent effects on brain beta-amyloid levels in PDAPP transgenic mice. J Neurosci 29:6771-6779.

Chalam KV, Grover S, Sambhav K, Balaiya S, Murthy RK (2014) Aqueous interleukin-6 levels are superior to vascular endothelial growth factor in predicting therapeutic response to bevacizumab in age-related macular degeneration. Journal of ophthalmology 2014:502174.

Chen M, Luo C, Penalva R, Xu H (2013) Paraquat-Induced Retinal Degeneration Is Exaggerated in CX3CR1-Deficient Mice and Is Associated with Increased Retinal Inflammation. Invest Ophthalmol Vis Sci 54:682-690.

Chen W et al. (2010) Genetic variants near TIMP3 and high-density lipoprotein-associated loci influence susceptibility to age-related macular degeneration. Proc Natl Acad Sci U S A 107:7401-7406.

Chinnery HR, McLenachan S, Humphries T, Kezic JM, Chen X, Ruitenberg MJ, McMenamin PG (2011) Accumulation of murine subretinal macrophages: effects of age, pigmentation and CX(3)CR1. Neurobiol Aging 33(8):1769-76..

Combadiere C, Feumi C, Raoul W, Keller N, Rodero M, Pezard A, Lavalette S, Houssier M, Jonet L, Picard E, Debre P, Sirinyan M, Deterre P, Ferroukhi T, Cohen SY, Chauvaud D, Jeanny JC, Chemtob S, Behar-Cohen F, Sennlaub F (2007) CX3CR1-dependent subretinal microglia cell accumulation is associated with cardinal features of age-related macular degeneration. J Clin Invest 117:2920-2928.

Dong LM, Weisgraber KH (1996) Human apolipoprotein E4 domain interaction. Arginine 61 and glutamic acid 255 interact to direct the preference for very low density lipoproteins. J Biol Chem 271:19053-19057.

Fryer JD, Demattos RB, McCormick LM, O'Dell MA, Spinner ML, Bales KR, Paul SM, Sullivan PM, Parsadanian M, Bu G, Holtzman DM (2005) The low density lipoprotein receptor regulates the level of central nervous system human and murine apolipoprotein E but does not modify amyloid plaque pathology in PDAPP mice. J Biol Chem 280:25754-25759.

Guo C, Otani A, Oishi A, Kojima H, Makiyama Y, Nakagawa S, Yoshimura N (2012) Knockout of ccr2 alleviates photoreceptor cell death in a model of retinitis pigmentosa. Exp Eye Res 104:39-47.

Gupta N, Brown KE, Milam AH (2003) Activated microglia in human retinitis pigmentosa, late-onset retinal degeneration, and age-related macular degeneration. Exp Eye Res 76:463-471.

Heeren J, Grewal T, Laatsch A, Becker N, Rinninger F, Rye KA, Beisiegel U (2004) Impaired recycling of apolipoprotein E4 is associated with intracellular cholesterol accumulation. J Biol Chem 279:55483-55492.

Hu SJ, Calippe B, Lavalette S, Roubeix C, Montassar F, Housset M, Levy O, Delarasse C, Paques M, Sahel JA, Sennlaub F, Guillonneau X (2015) Upregulation of P2RX7 in Cx3cr1-Deficient Mononuclear Phagocytes Leads to Increased Interleukin-1beta Secretion and Photoreceptor Neurodegeneration. J Neurosci 35:6987-6996.

499 Jonas JB, Tao Y, Neumaier M, Findeisen P (2010) Monocyte chemoattractant protein 1,
500 intercellular adhesion molecule 1, and vascular cell adhesion molecule 1 in exudative age-
501 related macular degeneration. Arch Ophthalmol 128:1281-1286.
502 Kezic JM, Chen X, Rakoczy EP, McMenamin PG (2013) The Effects of Age and Cx3cr1
503 Deficiency on Retinal Microglia in the Ins2Akita Diabetic Mouse. Invest Ophthalmol Vis
504 Sci 54:854-863.
505 Klaver CC, Kliffen M, van Duijn CM, Hofman A, Cruts M, Grobbee DE, van Broeckhoven
506 C, de Jong PT (1998) Genetic association of apolipoprotein E with age-related macular
507 degeneration. Am J Hum Genet 63:200-206.
508 Kohno H, Chen Y, Kevany BM, Pearlman E, Miyagi M, Maeda T, Palczewski K, Maeda A
509 (2013) Photoreceptor Proteins Initiate Microglial Activation via Toll-like Receptor 4 in
510 Retinal Degeneration Mediated by All-trans-retinal. J Biol Chem 288:15326-15341.
511 Koss MJ, Hoffmann J, Nguyen N, Pfister M, Mischak H, Mullen W, Husi H, Rejdak R, Koch
512 F, Jankowski J, Krueger K, Bertelmann T, Klein J, Schanstra JP, Siwy J (2014) Proteomics
513 of vitreous humor of patients with exudative age-related macular degeneration. PLoS One
514 9:e96895.
515 Lee S, Varvel NH, Konerth ME, Xu G, Cardona AE, Ransohoff RM, Lamb BT (2010)
516 CX3CR1 deficiency alters microglial activation and reduces beta-amyloid deposition in
517 two Alzheimer's disease mouse models. Am J Pathol 177:2549-2562.
518 Levy O, Calippe B, Lavalette S, Hu SJ, Raoul W, Dominguez E, Housset M, Paques M, Sahel
519 JA, Bemelmans AP, Combadiere C, Guillonneau X, Sennlaub F (2015) Apolipoprotein E
520 promotes subretinal mononuclear phagocyte survival and chronic inflammation in age-
521 related macular degeneration. EMBO Mol Med 7:211-226.
522 Liu J, Copland DA, Horie S, Wu WK, Chen M, Xu Y, Paul Morgan B, Mack M, Xu H,
523 Nicholson LB, Dick AD (2013) Myeloid cells expressing VEGF and arginase-1 following
524 uptake of damaged retinal pigment epithelium suggests potential mechanism that drives the
525 onset of choroidal angiogenesis in mice. PLoS One 8:e72935.
526 Luhmann UF, Carvalho LS, Robbie SJ, Cowing JA, Duran Y, Munro PM, Bainbridge JW, Ali
527 RR (2013) Ccl2, Cx3cr1 and Ccl2/Cx3cr1 chemokine deficiencies are not sufficient to
528 cause age-related retinal degeneration. Exp Eye Res 107:80-87.
529 Mahley RW, Rall SC, Jr. (2000) Apolipoprotein E: far more than a lipid transport protein.
530 Annu Rev Genomics Hum Genet 1:507-537.
531 Mahley RW, Weisgraber KH, Huang Y (2009) Apolipoprotein E: structure determines
532 function, from atherosclerosis to Alzheimer's disease to AIDS. J Lipid Res 50 Suppl:S183-
533 188.
534 Malek G, Johnson LV, Mace BE, Saloupis P, Schmechel DE, Rickman DW, Toth CA,
535 Sullivan PM, Bowes Rickman C (2005) Apolipoprotein E allele-dependent pathogenesis: a
536 model for age-related retinal degeneration. Proc Natl Acad Sci U S A 102:11900-11905.
537 Mattapallil MJ, Wawrousek EF, Chan CC, Zhao H, Roychoudhury J, Ferguson TA, Caspi RR
538 (2012) The rd8 mutation of the Crb1 gene is present in vendor lines of C57BL/6N mice
539 and embryonic stem cells, and confounds ocular induced mutant phenotypes. Invest
540 Ophthalmol Vis Sci. 53:2921-7
541 McKay GJ et al. (2011) Evidence of association of APOE with age-related macular
542 degeneration: a pooled analysis of 15 studies. Hum Mutat 32:1407-1416.
543 Ong JM, Zorapapel NC, Rich KA, Wagstaff RE, Lambert RW, Rosenberg SE, Moghaddas F,
544 Pirouzmanesh A, Aoki AM, Kenney MC (2001) Effects of cholesterol and apolipoprotein
545 E on retinal abnormalities in ApoE-deficient mice. Invest Ophthalmol Vis Sci 42:1891-
546 1900.

547 Penfold PL, Madigan MC, Gillies MC, Provis JM (2001) Immunological and aetiological
548 aspects of macular degeneration. Prog Retin Eye Res 20:385-414.
549 Peng B, Xiao J, Wang K, So KF, Tipoe GL, Lin B (2014) Suppression of microglial
550 activation is neuroprotective in a mouse model of human retinitis pigmentosa. J Neurosci
551 34:8139-8150.
552 Peri F, Nusslein-Volhard C (2008) Live imaging of neuronal degradation by microglia reveals
553 a role for v0-ATPase a1 in phagosomal fusion in vivo. Cell 133:916-927.
554 Riddell DR, Zhou H, Atchison K, Warwick HK, Atkinson PJ, Jefferson J, Xu L, Aschmies S,
555 Kirksey Y, Hu Y, Wagner E, Parratt A, Xu J, Li Z, Zaleska MM, Jacobsen JS, Pangalos
556 MN, Reinhart PH (2008) Impact of apolipoprotein E (ApoE) polymorphism on brain ApoE
557 levels. J Neurosci 28:11445-11453.
558 Rosenfeld ME, Butler S, Ord VA, Lipton BA, Dyer CA, Curtiss LK, Palinski W, Witztum JL
559 (1993) Abundant expression of apoprotein E by macrophages in human and rabbit
560 atherosclerotic lesions. Arterioscler Thromb 13:1382-1389.
561 Rutar M, Natoli R, Provis JM (2012) Small interfering RNA-mediated suppression of Ccl2 in
562 Muller cells attenuates microglial recruitment and photoreceptor death following retinal
563 degeneration. J Neuroinflammation 9:221.
564 Sakurai E, Anand A, Ambati BK, van Rooijen N, Ambati J (2003) Macrophage depletion
565 inhibits experimental choroidal neovascularization. Invest Ophthalmol Vis Sci 44:3578-
566 3585.
567 Seddon JM, George S, Rosner B, Rifai N (2005) Progression of age-related macular
568 degeneration: prospective assessment of C-reactive protein, interleukin 6, and other
569 cardiovascular biomarkers. Arch Ophthalmol 123:774-782.
570 Sennlaub F, Auvynet C, Calippe B, Lavalette S, Poupel L, Hu SJ, Dominguez E, Camelo S,
571 Levy O, Guyon E, Saederup N, Charo IF, Rooijen NV, Nandrot E, Bourges JL, Behar-
572 Cohen F, Sahel JA, Guillonneau X, Raoul W, Combadiere C (2013) CCR2(+) monocytes
573 infiltrate atrophic lesions in age-related macular disease and mediate photoreceptor
574 degeneration in experimental subretinal inflammation in Cx3cr1 deficient mice. EMBO
575 Mol Med 5:1775-1793.
576 Smoak KA, Aloor JJ, Madenspacher J, Merrick BA, Collins JB, Zhu X, Cavigiolio G, Oda
577 MN, Parks JS, Fessler MB (2010) Myeloid differentiation primary response protein 88
578 couples reverse cholesterol transport to inflammation. Cell metabolism 11:493-502.
579 Sullivan PM, Mezdour H, Aratani Y, Knouff C, Najib J, Reddick RL, Quarfordt SH, Maeda N
580 (1997) Targeted replacement of the mouse apolipoprotein E gene with the common human
581 APOE3 allele enhances diet-induced hypercholesterolemia and atherosclerosis. J Biol
582 Chem 272:17972-17980.
583 Sullivan PM, Han B, Liu F, Mace BE, Ervin JF, Wu S, Koger D, Paul S, Bales KR (2011)
584 Reduced levels of human apoE4 protein in an animal model of cognitive impairment.
585 Neurobiol Aging 32:791-801.
586 Suzuki M, Tsujikawa M, Itabe H, Du ZJ, Xie P, Matsumura N, Fu X, Zhang R, Sonoda KH,
587 Egashira K, Hazen SL, Kamei M (2012) Chronic photo-oxidative stress and subsequent
588 MCP-1 activation as causative factors for age-related macular degeneration. J Cell Sci
589 125:2407-2415.
590 Tsutsumi C, Sonoda KH, Egashira K, Qiao H, Hisatomi T, Nakao S, Ishibashi M, Charo IF,
591 Sakamoto T, Murata T, Ishibashi T (2003) The critical role of ocular-infiltrating
592 macrophages in the development of choroidal neovascularization. J Leukoc Biol 74:25-32.
593 Yu CE, Cudaback E, Foraker J, Thomson Z, Leong L, Lutz F, Gill JA, Saxton A, Kraemer B,
594 Navas P, Keene CD, Montine T, Bekris LM (2013) Epigenetic signature and enhancer
595 activity of the human APOE gene. Hum Mol Genet 22 :5036-47

Figure Legends:

Figure 1 : The APOE2 allele leads to age- and stress-related subretinal MP accumulation, retinal degeneration, and exacerbated choroidal neovascularization

A: Representative 12m-old IBA-1 stained RPE-flatmounts of *TRE3 and TRE2* mice and quantification of subretinal IBA-1$^+$MPs in 2m- and 12m-old mice of the indicated strains (n=9-20/group ANOVA/Dunnetts multiple comparison test at 12m versus *TRE3* control * $p<0.0001$)

B: Quantification of subretinal IBA-1$^+$MPs after a four day light-challenge followed by 10days of normal light conditions (d14) of 2m-old mice of the indicated strains (n= 14-16/group ANOVA/ Dunnetts Multiple Comparison at 14d versus *TRE3* control * $p<0.0001$).

C: Micrographs, taken 1000 µm from the optic nerve of 12m-old TRE3- and TRE2-mice. (C'): Photoreceptor nuclei rows at increasing distances (-3000µm: inferior pole, +3000µm: superior pole) from the optic nerve (0µm) in 12m-old mice. (C''): Quantification of the area under the curve of photoreceptor nuclei row counts of 2m- and 12m-old transgenic mouse strains (n=4-7; ANOVA/ Dunnetts Multiple Comparison at 12m versus *TRE3* control * p=0.0102) Mice were taken from several (≥3) independent cages for the quantifications.

D: CD102 (red) and IBA-1 (green) immunohistochemistry and quantification of subretinal IBA-1$^+$MPs on the RPE counted at a distance of 0-500µm to CD102$^+$CNV 7 days after the laser-injury of 2m-old mice of the indicated strains (n= 8-10/group ANOVA/ Dunnetts Multiple Comparison *$p<0.0001$).

E: CD102 immunohistochemistry and quantification of CD102 area on RPE/choroidal flatmount from 2m-old transgenic strains, 7 days after laser injury. (n=8-10/group; One-way ANOVA/ Dunnetts Multiple Comparison test * $p<0.0001$)

TRE2-4: Targeted replacement mice expressing human APOE isoforms ONL: outer nuclear layer; Scale bar Scale bar A, C, D, and E = 50µm.

Figure 2: The APOE2-allele increases APOE levels in the eye and APOE transcription and IIRC activation in MPs.

A: APOE ELISA of homogenates of PBS-perfused posterior segments of 12-month-old TRE2, TRE3, and TRE4 mice (n=5-6/group; One way ANOVA/Dunnetts Multiple Comparison test versus *TRE3* control * and ‡ $p<0.0027$).

B: Immunohistochemistry of APOE (red, upper panel), and IBA-1 (green, lower panel) of the subretinal side of a retinal flatmount from a 12m-old *TRE2*-mouse (representative of 3 independent experiments, experiments omitting the primary antibody immunostaining served as negative controls).

C : Quantitative RT–PCR of ApoE mRNA normalized with S26 mRNA of liver extracts from transgenic replacement mice expressing human APOE isoforms (TRE2-, TRE3-, TRE4-mice, n=3).

D : ELISA quantification of APOE plasma concentrations in transgenic replacement mice expressing human APOE isoforms (*TRE2*-, *TRE3*-, *TRE4*-mice, n=3 ; ANOVA/ Dunnetts Multiple Comparison versus *TRE3* control * $p<0.0001$).

E : Quantitative RT–PCR of *ApoE* mRNA normalized with *S26* mRNA of bone marrow derived monocytes from transgenic replacement mice expressing human APOE isoforms (*TRE2*-, *TRE3*-, *TRE4*-mice) cultured for 3d with or without porcine photoreceptor outer

segments to simulate subretinal monocyte to macrophage differentiation (n = 6/group; ANOVA/ Dunnetts Multiple Comparison Mo+POS versus *TRE3* control * p=0.0033).
F and G: Quantitative RT-PCR of *ApoE* mRNA normalized with *S26* mRNA (C, n=6; ANOVA/Dunnetts multiple comparison test versus *TRE3* control * p<0.0001) and APOE-ELISA of supernatants (D, n=6; ANOVA/Dunnett's multiple comparison test versus *TRE3* control * p<0.0001) of peritoneal Mϕs from *TRE*-mice cultured for 24h.
H: Human IL-6 ELISA of supernatants from human monocytes incubated for 24h in control medium, APOE3 (5µg/ml), heat-denaturated APOE3 (dAPOE3, 5µg/ml), APOE3 (5µg/ml) and Polymyxin B (25µg/ml), APOE3 (5µg/ml) and rat IgG1 isotype or human IgA2 isotype control, or mouse IgG1 isotype control, or rat anti-CD14 IgG1 antibody, or human anti-TLR4 IgGA2 antibody, or mouse anti-TLR2 IgG1 antibody (all antibodies at 25µg/ml) (n=4-6/group; One way ANOVA/Bonferroni multi-comparison tests: *APOE3 vs. CTL p<0.0001; # dAPOE3 vs. APOE3 p<0.0001; # APOE3 IgG vs APOE3 aCD14 Ab p<0.0001; # APOE3 IgG vs APOE3 aTLR4 Ab p<0.0001; # APOE3 IgA vs APOE3 aTLR2 Ab p<0.0001).
I: Quantitative RT-PCR of *IL-6, CCL2,* and *IL1β* mRNA normalized with *S26* mRNA (n=6; ANOVA/Dunnetts multiple comparison test versus *TRE3* control *IL-6**p=0.0069, *CCL2**p<0.0001, *IL1β**p=0.0097,) of peritoneal Mφs from *TRE*-mice cultured for 24h.
TRE2-4: Targeted replacement mice expressing human APOE isoforms; Scale bar B = 50µm.

Figure 3: IIRC-inhibition reduces subretinal MP accumulation and choroidal neovascularization in TRE2-mice in vivo.

A and B: 7d laser-injured IBA-1 (green) and CD102 (red) double-stained RPE-flatmounts of control IgG and anti-CD14 treated *TRE2*-mice. Quantification of subretinal IBA-1^+MPs/impact localized on the lesion surrounding RPE (G) and quantification of $CD102^+$ CNV area (H) of *TRE2*-mice treated with control IgG or CD14- blocking antibodies (intraocular antibody concentration 5µg/ml; n=12/group. Mann & Whitney t test G*p=0.0012; H*p=0.0009)
TRE2-4: Targeted replacement mice expressing human APOE isoforms; Scale bar B, G, and H = 50µm.

Figure 4: The APOE4-allele protects APOE-overexpressing $Cx3cr1^{GFP/GFP}$mice from subretinal MP accumulation, retinal degeneration and exacerbated choroidal neovascularization.

A: Representative 12m-old IBA-1 stained RPE-flatmounts of $Cx3cr1^{GFP/GFP}$*TRE3*-mice and $Cx3cr1^{GFP/GFP}$*TRE4*-mice and quantification of subretinal IBA-1^+MPs in 2m- and 12m-old mice of the indicated strains (n=8-13/group Mann & Whitney t test at 12 months*p=0.0034)
B: Quantification of subretinal IBA-1^+MPs after a four day light-challenge followed by 10days of normal light conditions (d14) of 2m-old mice of the indicated strains (n= 18/group Mann & Whitney t test at d14*p=0.0036).
C: Micrographs, taken 1000 µm from the optic nerve of 12m-old $Cx3cr1^{GFP/GFP}$*TRE3*-mice and $Cx3cr1^{GFP/GFP}$*TRE4*-mice. (C'): Photoreceptor nuclei rows at increasing distances (-3000µm: inferior pole, +3000µm: superior pole) from the optic nerve (0µm) in 12m-old mice. (C''): Quantification of the area under the curve of photoreceptor nuclei row counts of 12m-old transgenic mouse strains (n=9-5; Mann & Whitney t test *p=0.0032) Mice were taken from several (≥3) independent cages for the quantifications.
D: CD102 (red) and IBA-1 (green) immunohistochemistry and quantification of subretinal IBA-1^+MPs on the RPE counted at a distance of 0-500µm to $CD102^+$CNV 14 days after

the laser-injury of 2m-old mice of the indicated strains (n= 7/group Mann & Whitney t test *p=0.0182).
E: CD102 immunohistochemistry and quantification of CD102 area on RPE/choroidal flatmount from 2m-old transgenic strains, 14 days after laser injury. (n=7/group; Mann & Whitney t test *p=0.0034)
ONL: outer nuclear layer; Scale bar A, C, D, and E = 50µm.

Figure 5: The APOE4-allele decreases ocular APOE levels in Cx3cr1$^{GFP/GFP}$ mice and activates the IIRC inefficiently.
A: APOE ELISA of homogenates of PBS-perfused posterior segments of 12-month-old *Cx3cr1$^{GFP/GFP}$TRE3*-mice and *Cx3cr1$^{GFP/GFP}$TRE4*-mice (n=11-8/group Mann & Whitney t test *p=0.0276).
B: Human IL-6 and CCL2 ELISA of supernatants from human monocytes incubated for 24h in control medium, APOE3 (5µg/ml), or APOE4 (5µg/ml) (n=6; One way ANOVA/Bonferroni multi-comparison tests p<0.0001 for *IL-6* and *CCL2*, *p<0,05 different from control, ‡p<0.05 different from APOE3).
C and D: Quantitative RT-PCR of *ApoE* mRNA normalized with *S26* mRNA (C, n=4) and APOE-ELISA of supernatants (D, n=4) of peritoneal Mϕs from *TRE*-mice cultured for 24h.
E: Quantitative RT-PCR of *IL-6* and *CCL2* mRNA normalized with *S26* mRNA (n=5-10; Mann & Whitney t test ‡ *IL-6* p=0,0121, and *CCL2* p=0,0035) of peritoneal Mϕs from *TRE*-mice cultured for 24h.

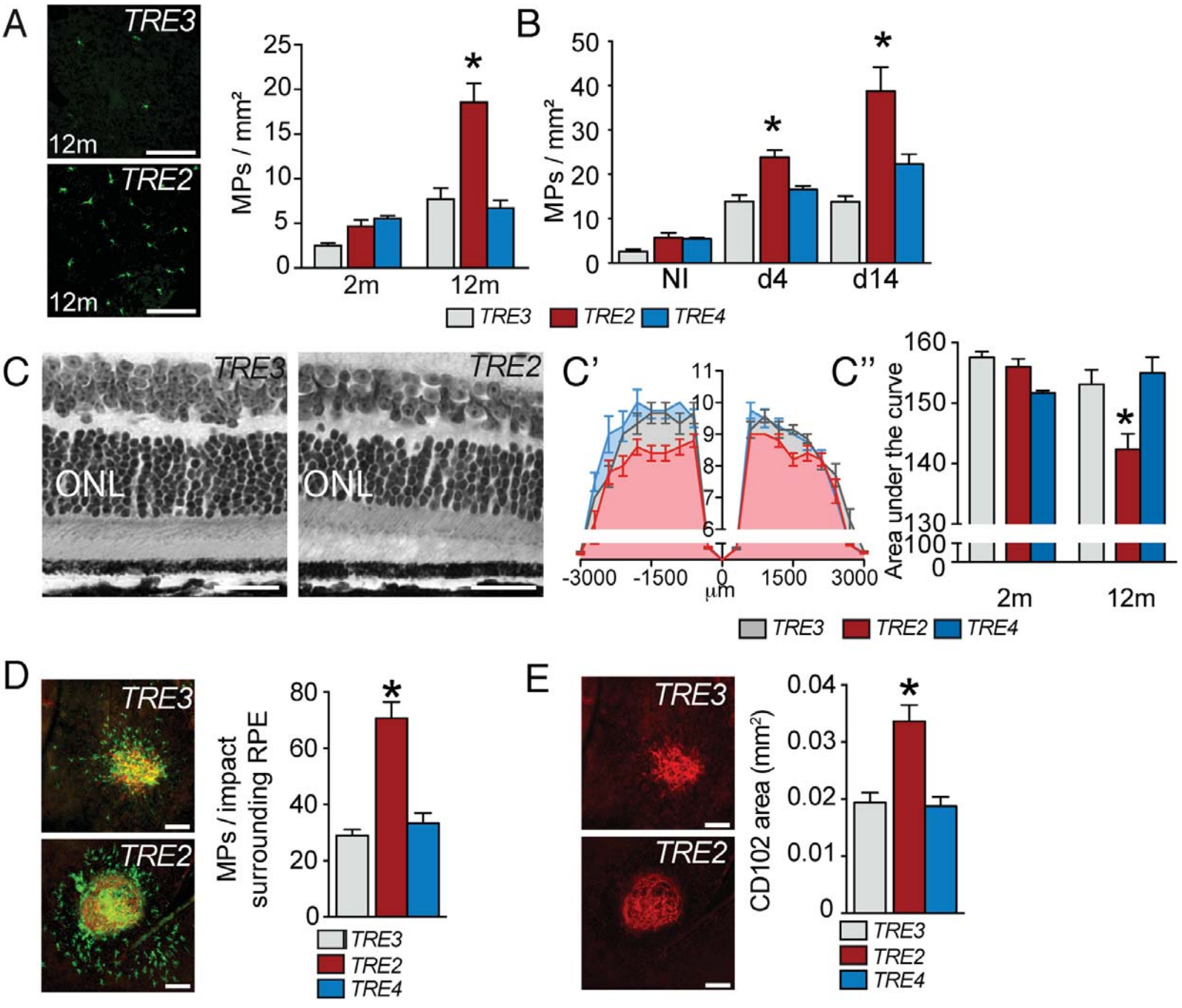
A
TRE3
12m
TRE2
12m
MPs / mm²
25
20
15
10
5
0
*
2m
12m
B
MPs / mm²
50
40
30
20
10
0
*
*
NI
d4
d14
TRE3
TRE2
TRE4
C
TRE3
TRE2
ONL
ONL
C'
11
10
9
8
7
6
-3000
-1500
0
1500
3000
µm
C''
Area under the curve
160
150
140
130
100
0
*
2m
12m
TRE3
TRE2
TRE4
D
TRE3
TRE2
MPs / impact surrounding RPE
80
60
40
20
0
*
TRE3
TRE2
TRE4
E
TRE3
TRE2
CD102 area (mm²)
0.04
0.03
0.02
0.01
0
*
TRE3
TRE2
TRE4

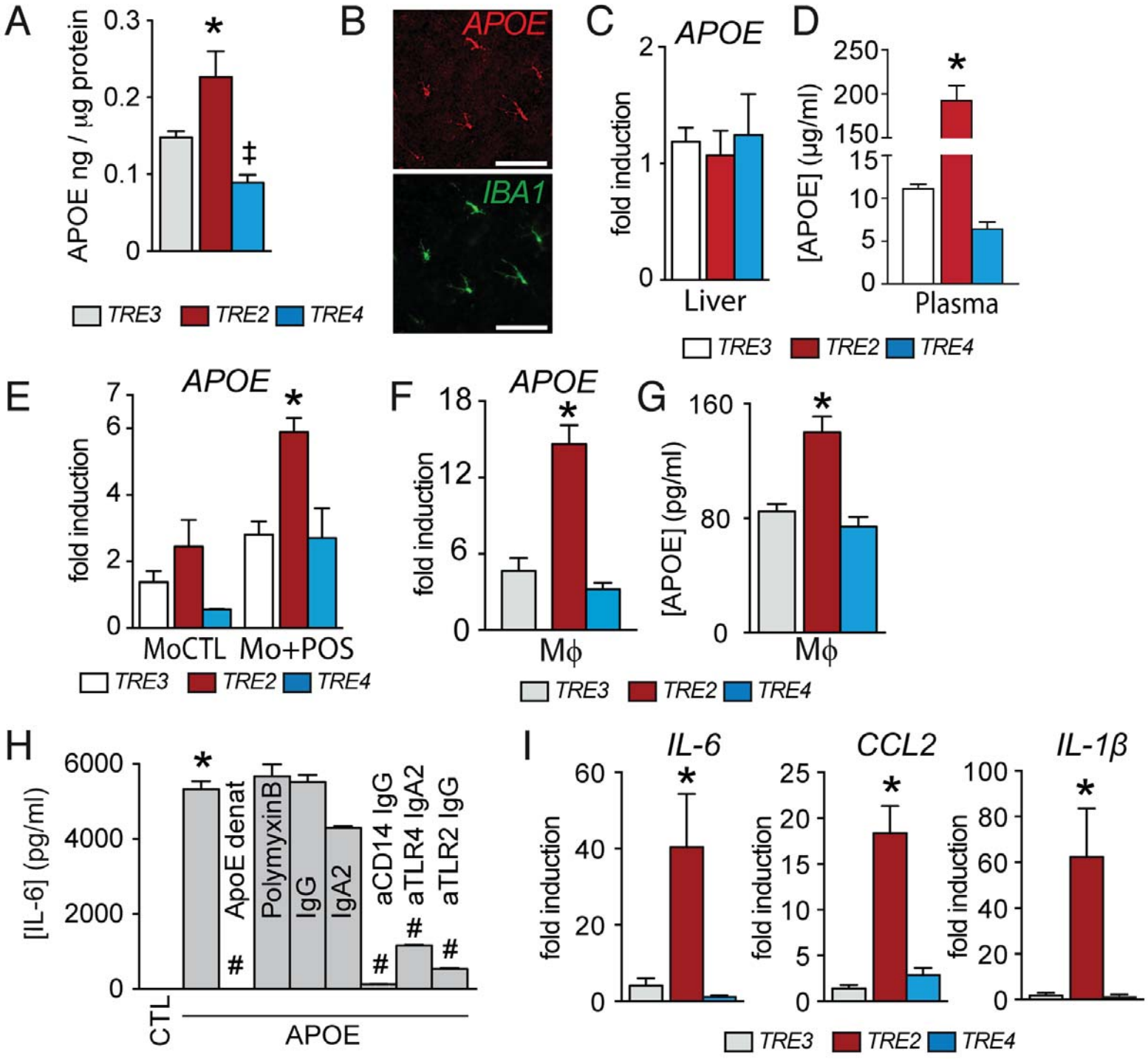
A
APOE ng / µg protein
0.3
0.2
0.1
0
*
‡
TRE3
TRE2
TRE4
B
APOE
IBA1
C
APOE
fold induction
2
1
0
Liver
D
[APOE] (µg/ml)
250
200
150
15
10
5
0
Plasma
E
APOE
fold induction
7
6
4
2
0
MoCTL
Mo+POS
F
APOE
fold induction
18
12
6
0
Mϕ
G
[APOE] (pg/ml)
160
80
0
Mϕ
H
[IL-6] (pg/ml)
6000
4000
2000
0
CTL
APOE
ApoE denat
PolymyxinB
IgG
IgA2
aCD14 IgG
aTLR4 IgA2
aTLR2 IgG
I
IL-6
CCL2
IL-1β
fold induction
60
40
20
0
25
20
15
10
5
100
80
60
40

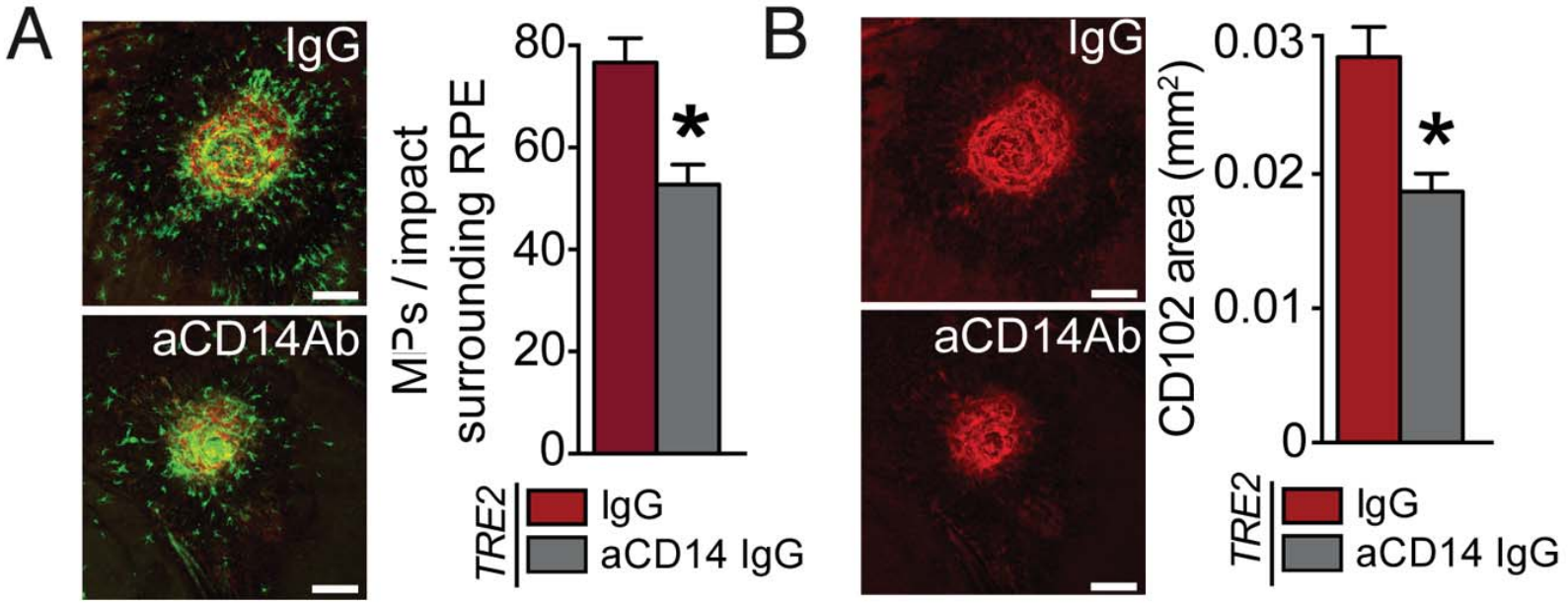
A
IgG
aCD14Ab
MPs / impact surrounding RPE
80
60
40
20
0
*
TRE2
IgG
aCD14 IgG
B
IgG
aCD14Ab
CD102 area (mm²)
0.03
0.02
0.01
0
*
TRE2
IgG
aCD14 IgG

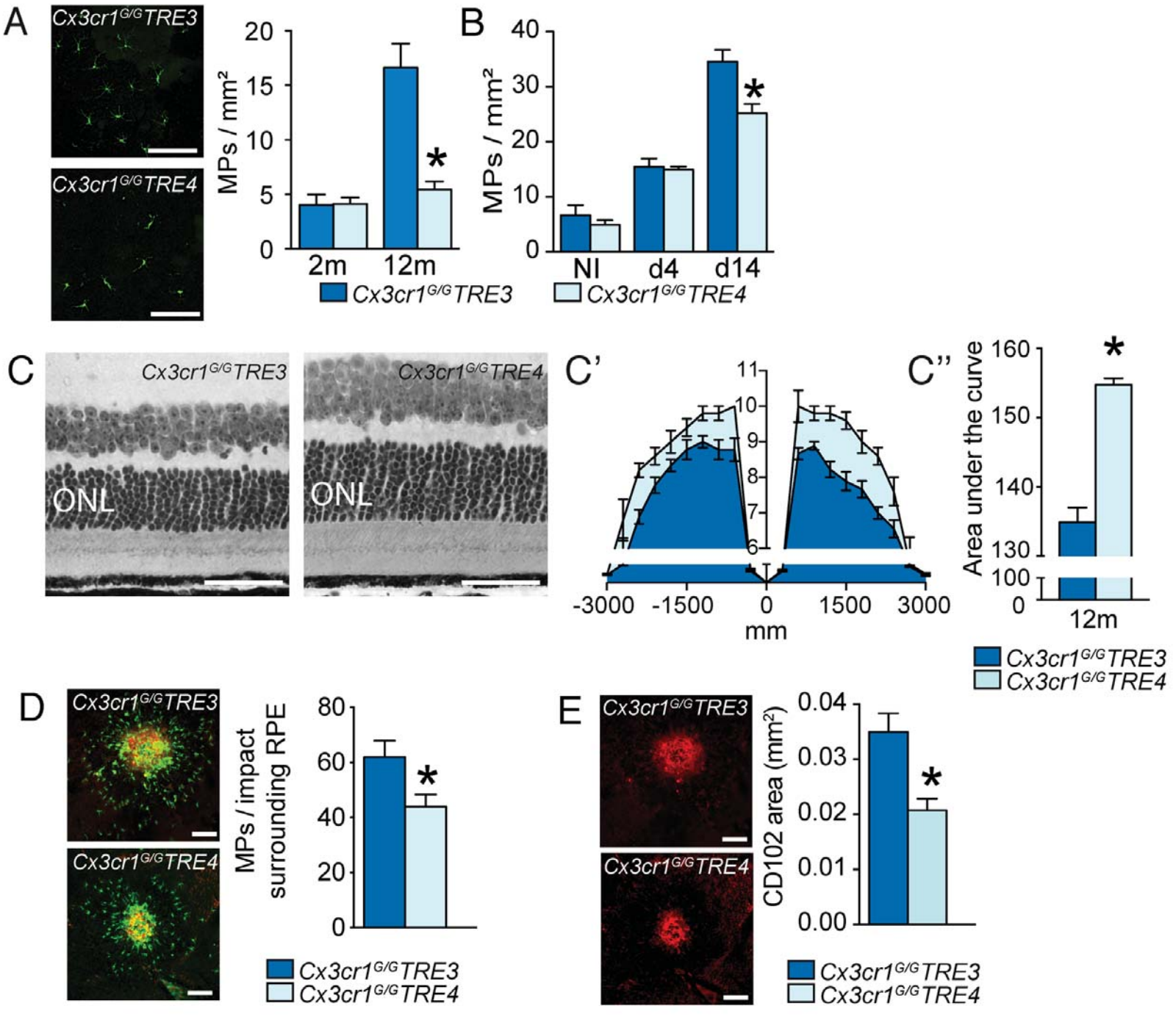
A
Cx3cr1G/GTRE3
Cx3cr1G/GTRE4
MPs / mm²
20
15
10
5
0
2m
12m
*
Cx3cr1G/GTRE3
B
MPs / mm²
40
30
20
10
0
Nl
d4
d14
*
Cx3cr1G/GTRE4
C
Cx3cr1G/GTRE3
Cx3cr1G/GTRE4
ONL
ONL
C'
11
10
9
8
7
6
-3000
-1500
0
1500
3000
mm
C''
Area under the curve
160
150
140
130
100
0
*
12m
Cx3cr1G/GTRE3
Cx3cr1G/GTRE4
D
Cx3cr1G/GTRE3
Cx3cr1G/GTRE4
MPs / impact surrounding RPE
80
60
40
20
0
*
Cx3cr1G/GTRE3
Cx3cr1G/GTRE4
E
Cx3cr1G/GTRE3
Cx3cr1G/GTRE4
CD102 area (mm²)
0.04
0.03
0.02
0.01
0.00
*
Cx3cr1G/GTRE3
Cx3cr1G/GTRE4

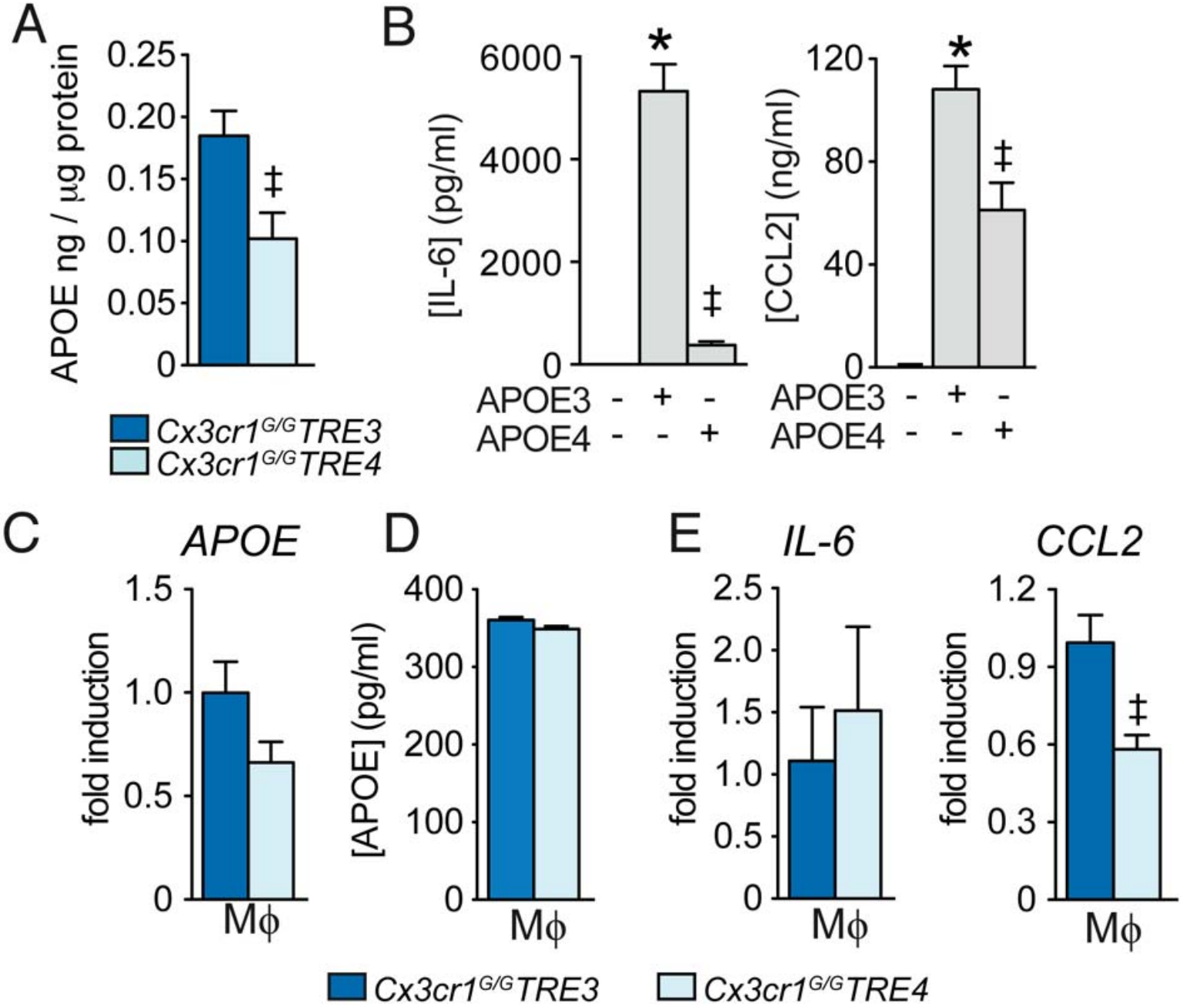
A
APOE ng / μg protein
0.25
0.20
0.15
0.10
0.05
0
‡
Cx3cr1G/GTRE3
Cx3cr1G/GTRE4
B
[IL-6] (pg/ml)
6000
4000
2000
0
*
‡
APOE3 - + -
APOE4 - - +
[CCL2] (ng/ml)
120
80
40
0
*
‡
APOE3 - + -
APOE4 - - +
C
APOE
fold induction
1.5
1.0
0.5
0
Mϕ
D
[APOE] (pg/ml)
400
300
200
100
0
Mϕ
E
IL-6
fold induction
2.5
2.0
1.5
1.0
0.5
0
Mϕ
CCL2
fold induction
1.2
0.9
0.6
0.3
0
‡
Mϕ
Cx3cr1G/GTRE3
Cx3cr1G/GTRE4